Experimental procedure for laboratory studies of in-situ burning - flammability and burning efficiency of crude oil

TITLE:

Experimental Procedure for Laboratory Studies of *in Situ* Burning – Flammability and Burning Efficiency of Crude Oil

AUTHORS AND AFFILIATIONS:
Laurens van Gelderen[1], Grunde Jomaas[1,2]

[1]Department of Civil Engineering, Technical University of Denmark, Kgs. Lyngby, Denmark
[2]School of Engineering, BRE Centre for Fire Safety Engineering, University of Edinburgh, Edinburgh, United Kingdom

CORRESPONDING AUTHOR:
Laurens van Gelderen (lauge@byg.dtu.dk)
Tel: (0045) – 4525 1808

EMAIL ADDRESSES:
Laurens van Gelderen (lauge@byg.dtu.dk)
Grunde Jomaas (Grunde.Jomaas@ed.ac.uk)

KEYWORDS:
In Situ Burning, Crude Oil, Weathering, Heat Transfer, Flammability, Burning Efficiency

SUMMARY:
Here, we present a protocol to simultaneously study the flammability and burning efficiency of fresh and weathered crude oil under conditions that simulate *in situ* burning operations on the sea.

ABSTRACT:
A new method for the simultaneous study of the flammability and burning efficiency of fresh and weathered crude oil through two experimental laboratory setups is presented. The experiments are easily repeatable compared to operational scale experiments (pool diameter ≥2 m), while still featuring quite realistic *in situ* burning conditions of crude oil on water. Experimental conditions include a flowing water sub-layer that cools the oil slick and an external heat flux (up to 50 kW/m^2) that simulates the higher heat feedback to the fuel surface in operational scale crude oil pool fires. These conditions enable a controlled laboratory study of the burning efficiency of crude oil pool fires that are equivalent to operational scale experiments. The method also provides quantitative data on the requirements for igniting crude oils in terms of the critical heat flux, ignition delay time as a function of the incident heat flux, the surface temperature upon ignition, and the thermal inertia. This type of data can be used to determine the required strength and duration of an ignition source to ignite a certain type of fresh or weathered crude oil. The main limitation of the method is that the cooling effect of the flowing water sub-layer on the burning crude oil as a function of the external heat flux has not been fully quantified. Experimental results clearly showed that the flowing water sub-layer does improve how

representative this setup is of *in situ* burning conditions, but to what extent this representation is accurate is currently uncertain. The method nevertheless features the most realistic *in situ* burning laboratory conditions currently available for simultaneously studying the flammability and burning efficiency of crude oil on water.

INTRODUCTION:

In situ burning of spilled crude oil on water is a marine oil spill response method that removes the spilled oil from the water surface by burning it and converting it to soot and gaseous combustion products. This response method was successfully applied during the Exxon Valdez[1] and Deepwater Horizon[2] oil spills and is regularly mentioned as a potential oil spill response method for the Arctic[3-6]. Two of the key parameters that determine whether *in situ* burning of oil will be successful as a spill response method are the flammability and the burning efficiency of the oil. The first parameter, flammability, describes how easily a fuel can be ignited and can lead to flame spreading over the fuel surface to result in a fully developed fire. The second parameter, burning efficiency, expresses the amount of the oil (in wt%) that is effectively removed from the water surface by the fire. It is thus relevant to understand the flammability and the expected burning efficiency of different crude oils under *in situ* burning conditions.

The ignition of oil slicks on water for *in situ* burning purposes is commonly addressed as a practical problem, with qualitative discussions on ignition systems[5,7-9]. The practical approach to the ignition of spilled oil as a binary problem, and labelling oils either "ignitable" or "not ignitable" (*e.g.* Brandvik, Fritt-Rasmussen, *et al*. [10]) is, however, incorrect from a fundamental point of view. In theory, any fuel can be ignited given an appropriate ignition source. It is therefore relevant to quantify the ignition requirements for a wide range of different crude oil types to better understand the properties of a crude oil that would label it as "not ignitable". For this purpose, the developed method can be used to study the ignition delay time of an oil as a function of the incident heat flux, the critical heat flux of the oil and its thermal inertia, *i.e.* how difficult it is to heat up the oil.

In a previous study, we postulated that the main parameter that governs the burning efficiency is the heat feedback to the fuel surface[11], which is a function of the pool diameter. The theory explains the apparent pool size dependency of the burning efficiency based on laboratory studies reporting low burning efficiencies (32-80%)[8,12,13] and large scale studies (pool diameter ≥2 m) reporting high burning efficiencies (90-99%)[14-16]. The method discussed herein was designed to test the proposed theory. By subjecting small scale laboratory experiments to a constant external heat flux, the higher heat feedback for large scale pool fires can be simulated under controlled laboratory conditions. As such, the developed method allows studying the burning efficiency effectively as a function of the diameter by varying the external heat flux.

In addition to an external heat flux to simulate the larger scale of *in situ* burning operations, the experimental setups feature cooling of the oil slick by a cold-water flow, simulating the cooling effect of the sea current. The discussed method is furthermore compatible with both fresh and weathered crude oils. The weathering of crude oil describes the physical and chemical process that affect a crude oil once it is spilled on water, such as losses of its volatile components and

mixing with water to form water-in-oil emulsions (*e.g.,* AMAP [17]). Evaporation and emulsification are two of the main weathering processes that affect the flammability of crude oils[18] and protocols for simulating these weathering processes are therefore included in the discussed method.

Herein, we present a novel laboratory method that determines the flammability and burning efficiency of crude oil under conditions that simulate *in situ* burning operations on sea. Previous studies on the flammability and burning efficiency of crude oils featured both comparable and different methods. The flammability of fresh and weathered crude oils as a function of an external heat flux was studied on water[19] and under Arctic temperatures[20]. Burning efficiency studies typically focus on different types of fresh and weathered crude oils and environmental conditions at a fixed scale (*e.g.,* Fritt-Rasmussen, *et al*. [8,]Bech, Sveum, *et al*. [21]). A recent study on the burning of crude oils contained by chemical herders is, to the knowledge of the authors, the first to study the burning efficiency for small, intermediate, and large scale experiments under similar conditions[13]. Large scale experiments are, however, not readily available for parametric studies due to the extensive amount of time and resources required for conducting such experiments. The main advantage of the presented method over the previously mentioned studies is that it allows for simultaneously studying both the flammability and burning efficiency of crude oil under semi-realistic conditions. The combination of studying these two parameters for crude oils as a function of both different oil types and the (simulated) pool diameter through easily repeatable experiments was previously unfeasible in practice.

PROTOCOL:

This protocol makes use of two different experimental setups that are used in steps 4-8, as shown in the accompanying schematics. The first setup is the Crude Oil Flammability Apparatus (COFA) (**Figure 1** and **Figure 4**), which is a 1.0 × 1.0 × 0.50 m^3 metal water basin designed to conduct small scale *in situ* burning of crude oil experiments, as shown for example in Van Gelderen, Brogaard, *et al*.[22] The second setup is a cone heater[23] with a spark igniter that features a custom-made sample holder and a gas analyzer that measures the O_2, CO_2, and CO concentrations in the exhaust duct[24] (**Figure 2** and **Figure 3**). The technical specifications of these setups are described in additional detail in the **Supplementary Document**, which also includes photographs of the setups. Unless specified otherwise, data measurements (*e.g.,* temperatures, heat fluxes, or gas concentrations) are measured digitally through a multiplexer and data logger. The data loggers are operated with a digital data acquisition program. In the protocol, the phrase "start the data logger" includes all actions according to the program instructions, as provided by the manufacturer, that are required to start the acquisition of data.

1. General Handling of Crude Oil

1.1 For each fresh oil that will be studied, take a 5 mL sample and measure its density and viscosity at 25 °C in a viscometer. Store the rest of the oil at 5-10 °C in a closed glass bottle until further use.

CAUTION: Fresh crude oil is highly flammable and both crude oil and its vapors pose a moderate

to high health hazard. It is furthermore difficult to clean from skin or eyes with non-hazardous chemicals such as soap. Wear safety glasses and gloves when handling crude oil and work in a well-ventilated area.

1.2 At the start of each test session, take the crude oils that will be tested out of the cooled (5-10 °C) storage. Shake each oil container by hand for 1-2 min and let them heat up to room temperature prior to conducting experiments. Return the crude oils to the cooled storage between test sessions.

1.3 Clean any surfaces accidentally contaminated with crude oil using a volatile non-polar solvent (*e.g., n*-heptane).

2. Evaporative Weathering of Crude Oil by Bubbling Pressurized Air through the Oil

Note: This step is based on Stiver and Mackay[25] and Buist, Potter, *et al*. [26]

2.1 Drill a number of holes (*e.g.*, six with a diameter (D) of 5 mm) evenly distributed in the lid of a plastic container of 5-10 L and drill a single hole (*e.g.*, D = 8-10 mm) in one of the sides of the container near its top edge.

2.2 Make an O-ring (approximately D = 20 cm) with an attached open connection out of plastic tubes with an inner diameter (I.D.) of 4-6 mm and drill a number of holes (*e.g.*, six with D = 1 mm) evenly distributed along one side of the O-ring.

Note: Try to offset the vertical location of the holes in the lid from the holes in the O-ring to minimize the amount of crude oil being blown out of the container.

2.3 Connect the O-ring to a plastic tube (*e.g.,* I.D. of 4-8 mm) that goes through the side hole of the plastic container. This tube will be connected to a pressurized air system with a regulating valve and a pressure gauge.

2.4 Weigh the lid and the plastic container with the plastic O-ring separately and register their weight.

2.5 Weigh 2-4 L of crude oil (based on its density) in the container and register the weight.

2.6 Place the container under a fume hood and connect the O-ring to the pressurized air system. Bubble air through the oil at a pressure that is as high as possible (*e.g.,* 200 kPa) without blowing oil through the holes in the lid of the container.

2.7 Weigh the oil at the start and end of each working day to monitor when the desired evaporative weathering state (in wt% lost) is achieved (*e.g.,* 20 wt% lost compared to the initial weight). This can take from one day to over a week of continuous bubbling, depending on the oil type and air pressure. Each intermediate weight measurement is used to establish an

evaporation curve as a function of time, which helps with predicting the necessary evaporation time to reach the desired evaporative weathering state.

Note: After the first day, the crude oil can typically be left in the fume hood for several days (*e.g.* over the weekend) without losing any significant amount of mass when the pressurized air is closed.

2.8 Once the evaporation of the crude oil is finished, take a 5 mL sample of the oil and measure its density and viscosity at 25 °C in a viscometer. Store the rest of the oil at 5-10 °C in a closed glass bottle for further use. Clean the container, lid, and O-ring with a volatile non-polar solvent to remove any crude oil remains.

3. Emulsification of Crude Oil Using a Rotary Shaking Table

Note: This portion of the protocol has been modified from Daling, M., *et al*.[27]

3.1 Add a total of 900 mL of crude oil and fresh or salt water mixture to a 1 L glass bottle, with the amount of water matching the desired vol% in the emulsion. For example, an emulsion with 40 vol% water content consists of 540 mL of crude oil and 360 mL of water. It is advised to use evaporated crude oil, rather than fresh crude oil, to more accurately present the weathering processes of spilled oil on open water and create more stable emulsions.

Note: It is important that the bottle is not fully filled so that there is free space available for turbulent mixing of the oil and water.

3.2 Vigorously shake the water-oil mixture by hand for 1-2 min. Then place the glass bottle on a rotary shaking table and stir the water-oil mixture at 175 rpm for 20 h at room temperature.

Note: In order to prevent issues with the separation of the water layer from the emulsion, conduct the experiments with the emulsion on the same day as when the 20 h shaking period is completed.

3.3 Take a 5 mL sample of the emulsion after the 20 h shaking period and measure its density and viscosity at 25 °C in a viscometer.

3.4 If the emulsion is unstable (see below), place the emulsion back on the rotary shaking table and constantly shake the emulsion at 175 rpm between experiments. At the start of each experiment, manually stop the rotary shaking table, take the required amount of emulsion (step 7.5), and then return it to the rotary shaking table. Once all experiments have been conducted with the emulsion, stop the rotary shaking table and store the emulsion in cooled (5-10 °C) storage.

3.5 If the emulsion is stable, remove the emulsion from the rotary shaking table and let it rest at room temperature. Shake the emulsion vigorously for 1-2 min by hand prior to taking the

required amount of oil for each experiment. Once all experiments have been conducted with the emulsion, store it in cooled (5-10 °C) storage.

Note: For the purpose of this protocol, unstable emulsions are defined as emulsions that form a clearly visible water layer with several hours, *i.e.* before the end of a typical workday.

4. Reference *in Situ* Burning Experiments in the COFA (Figure 1) for the Calibration of the Water Cooling in the Cone Setup

4.1 Place a 5 cm high Pyrex glass cylinder and an I.D. of 16.3 cm (outer diameter of 16.9 cm) on a stand, with a combined height of 35-45 cm, in the center of the COFA. The shape of the holder is irrelevant as long as it allows for a free flow of water under the area covered by the Pyrex glass cylinder. Fill the COFA with fresh water (340-440 L) so that the water level is 1 cm below the edge of the Pyrex glass cylinder.

4.2 Place a propeller on one of the sides of the COFA directly facing the Pyrex glass cylinder. Turn on the propeller and adjust the vertical height and flow so that waves are just barely observable in the water inside the Pyrex glass cylinder. Register the vertical height and flow stance (*e.g.*, 1,000 L/h) and turn the propeller off before continuing the protocol.

Note: The propeller is used to create a current in the water body that effectively cools the water layer below the burning crude oil in order to prevent the boilover phenomenon[28,29]. The initially set flow and vertical height of the propeller may not cause sufficient cooling of the water sub-layer, and a boilover then still occurs.

Caution: A boilover is an explosive burning state with a significantly increased flame height, burning rate, and heat release rate during which oil droplets are being ejected from the fire[29-31]. Ensure that any vulnerable equipment is protected (*e.g.*, with aluminum foil) and keep personnel and equipment at an appropriate distance from the fire.

4.3 Weigh an amount of crude oil equivalent to a 5-mm thick oil slick in the Pyrex glass cylinder (*i.e.*, based on the density and a volume of 104 mL) in an aluminum dish.

4.4 Pour the crude oil on the water inside the Pyrex glass cylinder. Be careful not to spill oil outside the bottom of the cylinder by pouring the oil too fast. Weigh the aluminum dish again and register the actual weight of the crude oil poured inside the Pyrex glass cylinder.

4.5 Slowly add water to the COFA until the surface of the oil slick is 1-2 mm below the edge of the Pyrex glass cylinder. This height difference is important to prevent the oil from overflowing upon ignition.

4.6 Turn on the exhaust hood and the propeller. Then ignite the crude oil using a butane hand torch and measure the burning time from the moment of ignition to the moment of extinction with a stopwatch.

4.7 After the fire is extinguished naturally, collect the oil remaining on the water surface (known as the burn residue) using hydrophobic absorption pads with a known weight. Shake any collected water off before weighing the pads to determine the residua weight. The burning efficiency is then calculated using Eq. (1) and the burning rate is calculated by dividing the difference between the initial mass and residue mass by the burning time (in seconds).

$$\textit{Burning efficiency} = \frac{mass_{initial} - mass_{residue}}{mass_{initial}} \cdot 100\% \quad (1)$$

4.8 In cases where the fire results in a boilover, repeat protocol step 4 by draining water from the COFA until the water surface is again one centimeter below the Pyrex glass cylinder edge. Clean the edges of the Pyrex glass cylinder with a volatile, non-polar solvent. Then reduce the vertical distance between the propeller and the Pyrex glass cylinder and/or increase the flow stance of the propeller and repeat protocol steps 4.3 to 4.8.

4.9 In case the fire does not end with a boilover, use the calculated burning efficiency and burning rate in step 4.7 to calibrate the water cooling in the cone setup.

5. Calibration of the Water Cooling for the Cone Setup (Figure 2 and Figure 3).

5.1 Puncture a flexible plastic tube (4 mm I.D.) at one centimeter from its ending with a 1 mm thick K-Type thermocouple so that the thermocouple bead is suspended freely inside the tube. Fix the thermocouple with polytetrafluoroethylene (PTFE) tape and aluminum tape to ensure that the thermocouple does not move and that water does not leak from the puncture. Connect the thermocouple to a data logger.

5.1.1. Repeat step 5.1 for a tube with a stainless-steel tube adapter and insert the thermocouple directly below the tube adapter.

5.2 Place and fix the first plastic tube with its end with the thermocouple as far to the bottom of the cooling reservoir as possible. Connect the other end of the tube to the inlet of a peristaltic pump with an adjustable flow speed.

5.3 Connect a new plastic tube to the outlet of the peristaltic pump and connect the other end of this plastic tube to a stainless-steel tube adapter. Connect the tube adapter to a bellows-sealed valve and connect the bellows-sealed valve to the cone sample holder. Ensure that the connections do not leak water by using PTFE tape between the connections when necessary.

5.4 Connect the other side of the cone sample holder to a bellows-sealed valve, which is then connected to the tube adapter of the tube with a thermocouple below the adapter. The other end of this tube is placed and fixed at the top of the cooling reservoir so that the outflowing water returns to the cooling reservoir.

Note: Make sure that the inlet tube and outlet tube have sufficient spatial distance in the reservoir so that heated water is not directly recirculated, but gets to cool down in the reservoir prior to recirculating.

5.5 Place the sample holder with the connected tubes under the cone heater. Adjust the height of the holder so that the outer edge is 23 mm from the bottom of the cone heater. Make sure that the tubes are of sufficient length so that the sample holder can easily be placed under the cone heater once the sample holder contains the crude oil.

5.6 Fill the cooling reservoir with demineralized water and cool the water to a chosen temperature (*e.g.*, 12 °C). Open the bellows-sealed valves and start the water flow through the sample holder at a chosen flow (*e.g.*, 7 L/h). Shake the holder to remove any remaining air from the holder so that the holder gets completely filled with water.

5.7 Start the data logger and continuously monitor the temperature of the in- and outflowing water. Stop the pump once the outflowing water temperature has stabilized (this is typically a few degrees above the set reservoir temperature), close the bellows-sealed valves, and turn on the exhaust hood.

5.8 Place the sample holder on a load scale and tare the scale. Add an amount of oil to the sample holder that corresponds to a slick thickness of 10 mm (*i.e.*, based on the density and a volume of 95 mL). Then open the bellows-sealed valves and start the pump again.

5.9 Place the sample holder carefully under the cone heater and ignite the oil with a butane hand torch. Measure the burning time from the moment of ignition to the moment of extinction with a stopwatch.

Caution: When burning oils that contain water, either naturally or due to emulsification, a boilover may occur during the burning (see also step 4).

5.10 After the fire is extinguished, stop the pump, close the valves, disconnect the tubes, and place the sample holder on a tared scale. Register the weight of the holder including the burn residue.

5.11 Clean any burned oil residue from the holder with a volatile non-polar solvent. Weigh the cleaned holder again to determine the residue weight. Then calculate the burning efficiency and burning time as described in step 4.7.

5.12 In case the burning efficiency and burning rate match the results from protocol step 4, the water temperature and flow are now calibrated and can be used in the following protocol step. In case the burning efficiency and burning rate do not match the results from protocol step 4, choose a new reservoir temperature and/or new flow accordingly. Reconnect the tubes to the sample holder, open the valves, start the pump, shake the holder to remove any air, and then repeat steps 5.7-5.12.

Note: It may not be possible to match both the burning efficiency and the burning rate. For the purpose of the described protocol, the burning efficiency is more important and should be matched as accurately as possible. When testing multiple oils, the water temperature and flow can be calibrated for either one oil, or for each oil individually. While calibrating the water temperature and flow for each oil individually may simulate the oil burning on water more accurately, ignition delay time results of various oils (step 6) can be more readily compared when using a fixed water temperature and flow for every experiment.

6. Calibration of the Cone Heater (Figure 2-3).

6.1 Calibrate the correlation between the temperature of the cone heater and the heat flux output using a water-cooled heat flux gauge with a maximum capacity of 100 kW/m^2.

6.1.1. Place an aquarium pump in a bucket and fill the bucket with cold tap water so that the pump is fully submerged.

6.1.2. Connect the aquarium pump to the heat flux gauge with a plastic tube. Connect a second plastic tube to the heat flux gauge and fix the other end of the tube inside the bucket, slightly above the water surface, so that water flowing out of the tube can be easily observed. Turn on the pump and ensure that a steady flow of water is flowing through the heat flux gauge.

6.1.3. Turn on the exhaust hood and heat up the cone to 200 °C. Place the heat flux gauge (facing upwards) 25 mm below the center of the cone and connect the heat flux gauge to the data logger. Start the data logger, open the shutters, and measure the heat flux for 5-10 min until a stable heat flux reading is acquired, then stop the data acquisition and close the shutters.

6.1.4. Repeat step 6.1.3 at cone temperatures of 300, 400, 500, 600, 700, 720, 740, 760, 780, and 800 °C.

6.2 Determine the cone temperatures that correspond to heat fluxes of 3-50 kW/m^2 using the measured data points and assuming a linear correlation between data points.

7. Flammability Experiments of Crude Oil in the Cone Setup (Figure 2-3)

7.1 At the beginning of each test session, check with the heat flux gauge whether the cone temperature corresponding to a heat flux of 10 kW/m^2 still gives the correct reading (±5%). If so, proceed with the protocol. If not, repeat step 6 before continuing.

7.2 At the beginning of each test session, turn on the exhaust hood, turn on the gas analyzer, and calibrate the gas analyzer according to the specifications provided by its manufacturer.

7.3 Ensure that when the sample holder is placed under the cone, there is a distance of 23 mm between the bottom of the cone and the outer edge of the holder.

7.4 Heat up the cone to a temperature corresponding to a heat flux of 5 kW/m^2.

7.4.1. In the meantime, cool the water reservoir to the temperature found in step 5, connect the water tubes to the sample holder, open the valves, and start the pump at the flow found in step 5. Shake the sample holder to remove any air trapped inside the holder. Start the data logger and monitor the water temperature until the outflowing water temperature has stabilized.

7.4.2. Once both the cone and the sample holder stabilize at their respective set temperatures, stop the pump, close the valves of the sample holder, and disconnect the tubes from the valves.

7.5 Place the sample holder on a load scale and tare the scale. Add an amount of oil at room temperature to the sample holder that corresponds to a slick thickness of 10 mm (*i.e.,* based on the density and a volume of 95 mL). Then reconnect the tubes, open the bellows-sealed valves, and start the pump again.

7.6 Start the data logger for the gas analyzer to measure the O_2, CO_2, and CO concentrations in the combustion gases and the temperature of the in- and out-flowing water.

7.7 Carefully place the sample holder under the cone and ready two stopwatches. Move the spark igniter into position over the sample. Then open the shutters and start the first stopwatch.

7.8 Upon ignition of the oil, simultaneously stop the first stopwatch and start the second stopwatch. Then move the spark igniter back into its neutral position away from the burning sample.

7.8.1. If the oil does not ignite within 10 min, stop the first stopwatch and move the spark igniter back into its neutral position. Then ignite the oil using a butane hand torch and start the second stopwatch.

Caution: When burning oils that contain water, either naturally or due to emulsification, a boilover may occur during the burning (step 4).

7.9 After the fire is extinguished, stop the second stopwatch, close the shutters, and stop the data acquisition of the gas analyzer and cooling water temperatures. Then stop the pump, close the valves, disconnect the tubes, and place the sample holder on a tared scale. Register the weight of the holder including the burn residue.

7.10 Clean the holder from any burned oil residue with a volatile non-polar solvent. Weigh the cleaned holder again to determine the residue weight. Then calculate the burning efficiency and burning time as described in step 4.7.

7.11 For each oil that is to be tested, repeat steps 7.4-7.10 for heat fluxes of 10, 20, 30, 40, and 50 kW/m^2. Remove any soot deposited on the cone heater coil after each experiment.

7.11.1. In order to establish the minimum required heat flux needed for piloted ignition, *i.e.* the critical heat flux, it may be necessary to test additional heat fluxes. Repeat steps 7.4-7.10 for heat fluxes lowered by 1 kW/m^2 increments from the lowest heat flux at which piloted ignition occurred until a heat flux is tested for which piloted ignition is not observed within 10 min. The critical heat flux is then found within a 1 kW/m^2 upper range of this heat flux.

Caution: Very volatile crude oils can ignite spontaneously when subjected to very high heat fluxes (≥40 kW/m^2), even when the shutters of the cone heater are closed.

8. Surface Temperature upon Ignition Experiments of Crude Oil in the COFA Setup (Figure 4).

8.1 Place a 5-cm high Pyrex glass cylinder with an I.D. of 16.3 cm (O.D. of 16.9 cm) on a stand, with a combined height of 35-45 cm, in the center of the COFA (**Figure 1**). Place two infrared (IR) heaters mounted on adjustable stainless-steel footings on two opposite sides of the Pyrex glass cylinder at a horizontal distance of at least 5 cm from the outer edge of the cylinder.

Note: The precise specifications and dimensions of the IR heaters are irrelevant as long as they can provide a sufficiently high heat flux to the oil surface to ignite crude oils, which typically requires 5-20 kW/m^2 for ignition. A minimum power of 1 kW and minimum heater width of 17 cm are advised. Any cooling systems of the IR heaters, such as air fans, should furthermore not interact with the oil slick during the experiment.

8.2 To measure the surface temperature upon ignition of a crude oil, an incident heat flux of 2-5 kW/m^2 higher than its critical heat flux (step 7.11.1) is advised.

8.2.1. Prepare a 100 kW/m^2 heat flux gauge according to steps 6.1.1-6.1.2 and connect the heat flux gauge to a data logger. Place the heat flux gauge in the center of the Pyrex glass cylinder, facing upwards, at a height of 1-2 mm below the upper edge of the cylinder. The horizontal area at this height inside the Pyrex glass cylinder is from here on referred to as “the horizontal plane”. This horizontal plane corresponds to the surface of an oil slick inside the Pyrex glass cylinder.

Note: Ensure that the heat flux gauge can be freely moved in the horizontal plane so that it can measure the incident heat flux at various locations of the horizontal plane. The Pyrex glass cylinder only functions as a visual aid for correctly placing the heat flux gauge horizontal plane, so if necessary, the Pyrex cylinder can be removed during step 8.2.

8.2.2. Start the data logger, turn on the IR heaters, and monitor the incident heat flux at the center of the horizontal plane. Tune the incident heat flux to the horizontal plane by adjusting the spatial location of the IR heaters (height, angle, and horizontal distance from the horizontal plane) and their power output percentage until the desired incident heat flux is obtained.

8.2.3. Measure the incident heat flux at the outer edges of the horizontal plane. At all locations, the incident heat flux should be 2-5 kW/m^2 higher than the critical heat flux of the oil that will be tested. Adjust the location and power output percentage of the IR heaters according to the previous step, if necessary.

8.2.4. After each adjustment of the location and power output of the IR heaters, measure the incident heat flux to the horizontal plane at its center and the outer edges.

8.2.5. Repeat steps 8.2.2-8.2.5 until the measured incident heat flux throughout the horizontal plane is 2-5 kW/m^2 higher than the critical heat flux of the selected oil. Then, turn off the IR heaters and remove the heat flux gauge. Place the Pyrex glass cylinder back on its stand, if necessary.

8.3 Fill the COFA with fresh water (340-440 L) so that the water level is one centimeter below the edge of the Pyrex glass cylinder. Place a propeller on one of the sides of the COFA directly facing the Pyrex glass cylinder at the height found in step 4.

8.4 Place and fix a set of three 1 mm thick K-Type thermocouples at 1-2 mm below the edge of the Pyrex glass cylinder. Arrange the thermocouples so that they measure along the radius of the cylinder, with a distance of about 1-2 cm between each thermocouple. Connect the thermocouples to a data logger.

8.5 Attach a spark igniter with a metal clamp to a metal rod on a metal stand that stands in the COFA. Place the stand so that the igniter can easily be moved from a neutral position to a position 2-3 cm above central area of the Pyrex Glass Cylinder and back to its neutral position again.

8.6 Weigh an amount of crude oil equivalent to a 5-mm thick oil slick in the Pyrex glass cylinder (*i.e.,* based on the density and a volume of 104 mL) in an aluminum dish.

8.7 Pour the crude oil on the water inside the Pyrex glass cylinder. Be careful not to spill oil outside the bottom of the cylinder by pouring the oil too fast. Weigh the aluminum dish again and register the actual weight of the crude oil poured inside the Pyrex glass cylinder.

8.8 Slowly add water to the COFA until the surface of the oil just comes into contact with the three thermocouples. Move the spark igniter to its position above the oil.

8.9 Start the data logger and a stopwatch in sync so that each second matches a specific scan number. Turn on the exhaust hood, the propeller, and the spark igniter. Turn on the IR heaters and set the power output to the percentage found in step 8.2.

8.10 Upon ignition of the oil, stop the stopwatch and data logger, turn off the spark igniter, and move it to its neutral position and turn off the IR heaters and the propeller. Then extinguish

the fire by carefully placing a non-combustible cover over the Pyrex glass cylinder. Extinguishing the fire may require the thermocouples to be moved away first.

8.11 Collect and dispose of the crude oil with hydrophobic absorption pads. Drain water from the COFA until the water level is low enough to measure the incident heat flux to the horizontal plane again with a heat flux gauge. Clean the Pyrex glass cylinder with a volatile non-polar solvent.

8.12 Plot the temperature of the three thermocouples as a function of the scan number. Based on the time on the stopwatch, the corresponding scan number, and the plotted graph, determine the surface temperature upon ignition of the tested crude oil.

8.13 For each additional oil that will be tested, repeat steps 8.2-8.12.

REPRESENTATIVE RESULTS:

Figure 5 shows the evaporation curve of a light crude oil that was evaporated over multiple days to a loss of 30 wt% using the method described in step 2. The figure clearly shows that after the first day (19 h) of evaporative weathering, the evaporation rate is reduced significantly, which allows for pauses as mentioned in the protocol.

Figure 6 shows the ignition delay time as a function of the incident heat flux from the cone heater (step 7, **Figure 2-3**) for fresh Grane (a heavy crude oil) and evaporated Grane with losses of 7 wt%. The results give an example of the increased ignition delay times for evaporated crude oils. In addition, the critical heat flux, represented by the vertical asymptotes, also increases as a function of the evaporative losses. Overall, these results give an impression of the strength and exposure duration an ignition source needs to have in order to ignite these different types of crude oils. Additional results obtained with the protocol described herein can be found in Van Gelderen, Rojas Alva, *et al*.[32]

A more typical presentation of the ignition delay time as a function of the incident heat flux is shown in **Figure 7**. Crude oil slicks typically behave as thermally thick materials and the ignition delay time (t_{ig}) can then be described by Eq. (2)[19,32].

$$t_{ig} = \frac{\pi}{4} \cdot k\rho c \cdot \left(\frac{T_{ig} - T_{\infty}}{a \cdot \dot{q}''_{inc}} \right)^2 \tag{2}$$

Here, k is the thermal conductivity, ρ the density, c the specific heat coefficient, T_{ig} the surface temperature upon ignition, T_{∞} the ambient temperature (assumed to be 20 °C), a the absorptivity, and $\dot{q}''_{inc}$ the incident heat flux. Rewriting this equation gives the ignition delay time as a linear function of the incident heat flux (Eq. 3).

$$\frac{1}{\sqrt{t_{ig}}} = \frac{2}{\sqrt{\pi}} \cdot \frac{a}{\sqrt{k\rho c}} \cdot \frac{\dot{q}''_{inc}}{T_{ig} - T_{\infty}} \tag{3}$$

By plotting the ignition delay time in the form of $1/\sqrt{t_{ig}}$ as a function of the incident heat flux, the data should show a linear trend line, and as such allow for assessing the validity of the data. Furthermore, the slopes of the trend lines for different crude oils give an indication of their relative thermal inertias (*kpc*) because the lower the slope, the harder it is to heat up (and thus ignite) a crude oil.

The results for evaporated Grane (**Figure 7**) give a good example of a data set that fits with its linear trend line, with an R^2 value of 0.991. On the other hand, the results for fresh Grane clearly start to deviate from the linear trend at higher heat fluxes (30 kW/m^2). This behavior is most likely caused by the extremely short ignition delay times (<10 s) at such high heat fluxes for this type of volatile fuel. Fresh Grane, similar to other fresh crude oils, contains a high amount of volatile components that ignite very rapidly under high incident heat fluxes. One of the assumptions underlying Eq. (2) is that the time it takes for the combustible gases evaporating from the fuel to mix with oxygen and reach the spark igniter is negligible[33]. With ignition delay times of less than 10 seconds, however, this mixing time, which is estimated to be on the order of a few seconds, does become a significant contributor to the ignition delay time. Equation (2) is then no longer valid with these short ignition delay times, and hence the data deviates from the linear trend line. When studying the flammability of very volatile crude oils, this behavior should thus be taken into account when analyzing the ignition delay time data.

Figure 8 shows the heat release rates as a function of time for a fresh light crude oil and an emulsified light crude oil (prepared according to steps 2-3). The heat release rates are calculated with the O_2, CO_2, and CO concentration measurements from the gas analyzer (step 7) according to Eq. (26) from Janssens[34]. See the **Supplementary Document** for further details on these calculations. The fresh crude oil shows a typical heat release rate profile of a slowly decreasing heat release rate over time, which is representative of all crude oils that do not contain any water. The emulsified crude oil shows a good example of the explosiveness of the boilover phenomenon, with a heat release rate that rapidly increases up to a factor five times higher than the regular burning phase prior to boilover. Boilovers are highly irregular phenomena, though, and the intensity, duration, and time of occurrence depend on the stability and the volume percentage of the water inside the crude oil.

Figure 9 shows the burning efficiency and burning rate as a function of the incident heat flux for a fresh light crude oil and a heavy evaporated oil with losses of 7 wt%. Both the burning rate and burning efficiency increase with increasing incident heat flux for both crude oil types. At low heat fluxes, the burning efficiency shows a significant difference between the fresh light crude oil and the heavy evaporated crude oil. At higher heat fluxes, the burning efficiencies for these oils converge to similar values, which is typical behavior for all types of fresh and weathered crude oil. The burning rate does not show this converging trend for different oils, because the burning time also changes as a function of the incident heat flux, which can be different for each oil type. For crude oils containing water, the water fraction should in principle not be accounted for when calculating the burning efficiency and the burning rate because it is a non-combustible material. However, the water does evaporate during the burning and the onset of boilover further complicates burning efficiency and burning rate estimations as it propels oil and water droplets

from the fuel. As such, emulsified crude oils may thus display deviations from the data shown, for example in **Figure 9,** and care should be taken when analyzing burning efficiency and burning rate results of crude oils containing water.

Figure 10 shows the surface temperature of two thermocouples at the fuel surface as a function of time for an evaporated light crude oil with losses of 20 wt% in the COFA setup (step 8, **Figure 4**). The result shows a clear spike in temperature after 178 s. Right before this moment, the surface temperature of the crude oil is 129 °C as measured by both thermocouples, which is the surface temperature upon ignition. In combination with the ignition delay time results for this oil (step 7), Eq. (2) can then be used to calculate the thermal inertia for the oil. **Table 1** shows the thermal inertia values for this evaporated light crude oil based on its surface temperature upon ignition at 129 °C and its ignition delay times as a function of the incident heat flux. Wu, *et al*.[19] found that the absorptivity could not be set to unity for crude oils and this term was thus included in the thermal inertia calculations. Literature values of the thermal inertia for crude oils for comparison purposes can be found in Wu, *et al*.[19] and Ranellone, *et al*.[20]

FIGURE AND TABLE LEGENDS:

Figure 1: Schematics of the COFA setup. The schematics include a detailed view of the Pyrex glass cylinder on its stand (left), a top view of the COFA (middle), and a cross sectional view of the full setup (right). In addition, a set of three close-ups (a-c) show the filling process of the COFA that corresponds to protocol steps 4.1 (a), 4.4 (b), and 4.5 (c). The COFA setup is used in step 4 to determine the calibration points of the burning efficiency and burning rate of a crude oil for the cone setup.

Figure 2: Full schematic overview of the cone setup (not to scale). The setup consists of a cone heater with a control unit, a custom-made cone sample holder, a peristaltic pump and water cooling reservoir, and an exhaust hood with a gas analyzer. The schematics also feature a close-up of the thermocouple placement in the water tubes (step 5.1). This setup is used in step 7 to study the flammability of crude oils. Note that there is no direct contact between the oil and the cooling water in this setup, as they are separated by the metal holder. Details of the cone sample holder are given in **Figure 3**.

Figure 3: Detailed cross-sectional schematic of the circular sample holder of the cone setup. The metal edges prevent the oil from overflowing upon ignition and are angled 30° from the oil slick to minimize re-radiation. This cone sample holder is used in step 7 to study the flammability of crude oils. Note that there is no direct contact between the oil and the cooling water in this setup, as they are separated by the metal holder.

Figure 4: Schematics of the COFA setup for studying the surface temperature of crude oil upon ignition. The schematics show a top view (left) and cross-sectional view (right) and the setup includes infrared (IR) heaters, a spark igniter, and a set of three thermocouples to measure the surface temperature of the oil slick (step 8). Additional details of the COFA setup are shown in **Figure 1**.

Figure 5: Evaporative losses of a light crude oil (DUC) as a function of time. The data were obtained using the air bubbling method described in step 2 and clearly show a reduced evaporation rate after the first day (19 h).

Figure 6: Ignition delay time results as a function of the incident heat flux for a fresh and evaporated (loss of 7 wt%) heavy crude oil (Grane). These data were obtained using the cone setup (**Figure 2**) according to the protocol in step 7. The vertical asymptotes show the critical heat flux (4 and 7 kW/m^2) within a 1 kW/m^2 upper range. The error bars indicate a data range based on 2-3 experiments.

Figure 7: Ignition delay time results as a function of the incident heat flux for a fresh and evaporated (loss of 7 wt%) heavy crude oil (Grane). These data were obtained using the cone setup (**Figure 2**), according to the protocol in step 7, and processed with Eq. (2). The results indicate that the evaporated Grane has a higher thermal inertia than fresh Grane, as expected. The graph furthermore shows how, for volatile crude oils at high incident heat fluxes, very short ignition delay times (<10 s) can deviate from the linear trend line. The error bars indicate a data range based on 2-3 experiments.

Figure 8: Heat release rate as a function of time for a light fresh crude oil and an emulsified light crude oil with evaporated losses of 40 wt% and containing 40 vol% water. The data were obtained from the cone setup (**Figure 2**) by processing the O_2, CO_2, and CO concentration measurements from the gas analyzer (step 7) according to Eq. (26) from Janssens[34]. The fresh crude oil shows a regular heat release rate profile for crude oils without water content. The emulsified light crude oil resulted in a boilover at the end of the burn and its heat release profile gives an indication of the intensity of a boilover compared to a regular crude oil fire.

Figure 9: Burning efficiency and burning rate as a function of the incident heat flux for a fresh light crude oil (DUC) and an evaporated heavy crude oil with losses of 7 wt% (Grane 7%). The data were obtained in the cone setup (**Figure 2**) according to Step 7 and show how the burning efficiencies of different crude oil types converge at high incident heat fluxes. All data points had a maximum error of 2.5% from the shown averages.

Figure 10: Surface temperature as a function of time for two thermocouples during an ignition experiment in the COFA with an evaporated light crude oil with losses of 20 wt%. The data were obtained in the COFA setup (**Figure 4**) according to the protocol in Step 8. The sudden spike in temperature after 178 s indicates the moment of ignition. The temperature right before this sudden temperature spike shows the surface temperature upon ignition.

Table 1: Ignition delay times and corresponding thermal inertia as a function of the incident heat flux for an evaporated light crude oil with losses of 20 wt%. The thermal inertia is calculated using Eq. (2), based on the ignition delay time data obtained in step 7 and the surface temperature upon ignition data in step 8.

DISCUSSION:

The two weathering methods discussed in this paper are a relatively simple approximation of the weathering processes that a spilled oil on water is subjected to[17]. Other, more sophisticated weathering methods can also be used to provide weathered crude oil samples, such as the circulating flume described by Brandvik and Faksness[35]. The advantage of the presented methods is that they require simple equipment and can be easily conducted in a laboratory environment. The resulting weathered crude oils are then functional for the purposes of the flammability and burning efficiency studies in this protocol, as demonstrated in the Representative Results section.

One of the main limitations in the protocol is the calibration of the water cooling for the cone setup (step 5). The issue is that there is no reference data available for *in situ* burning field experiments at the same scale and under similar conditions as the cone setup. There are furthermore no readily available heat transfer models that can be used in practice to determine the heat balance between a burning crude oil and its flowing water sub-layer. The water cooling calibration therefore has to be based on experimental data from the COFA setup (step 4). As mentioned in the protocol, the calibration can then be conducted for either single oils or for each oil separately. Without reference data or a suitable heat transfer model, it is impossible to know which of these methods, if any, gives a correct representation of the heat balance for *in situ* burning of crude oil on water.

The heat balance in the cone setup is further complicated by subjecting the crude oil to an external heat flux, which may also affect the cooling capacity of the water that flows through the cone sample holder. During the burning of a crude oil under the cone heater, the outflowing water increases in temperature over time, the extent of which depends on the incident heat flux. At the maximum incident heat flux of 50 kW/m^2, the water was even observed to be boiling, as steam came out of the water outlet. It is currently unclear to what extent the cooling water is directly heated by the cone heater (and not the burning oil) and whether it has a significant effect on the results. Only through an extensive empirical experimental study would it be possible to optimize the water cooling calibration for all tested incident heat fluxes and for each tested oil type. Despite these issues, implementing the water cooling in the cone setup undoubtedly improved the capability of the cone setup to represent *in situ* burning conditions. Preliminary experiments with a sample holder without water cooling failed to reproduce the low burning efficiencies observed in the COFA and could not be used to represent the *in situ* burning of crude oil. The discussed limitation is thus not a matter of whether the current cone setup represents *in situ* burning conditions of crude oil on water, but to which extent it correctly represents those conditions. As far as we are aware, the presented laboratory procedure is, despite this limitation, currently the most realistic method for studying the flammability and the burning efficiency of *in situ* burning of crude oil on water.

A critical step in the protocol is the measurement of the surface temperature upon ignition in the COFA setup (Step 8). It is very important that when the propeller is turned on, the surface of the oil slick inside the Pyrex glass cylinder is as still as it can be. If the oil surface is too much in (vertical) motion, the location and the flow of the propeller (step 4) should be adjusted to reduce the turbulence at the oil surface. Without a still oil surface, it becomes very challenging to

accurately measure the surface temperature upon ignition in step 8. The choice of IR heaters is also critical to the success of this step. During the development of this protocol, it was found that the IR heaters need to have a very high radiation output, while being as compact as possible and have a cooling system that does not interfere with the temperature measurements. It is thus important to carefully select a set of IR heaters for the COFA setup in **Figure 4**. Ideally, the IR heaters need to be able to provide a heat flux of at least 15 kW/m^2 at distances much further away than 5 cm from the Pyrex glass cylinder. This would allow using the IR heaters while the crude oil is burning. The burning efficiency of crude oils can then be tested as a function of an incident heat flux in an experimental setup that better represents *in situ* burning conditions.

Further improvements to the representation of *in situ* burning conditions during the flammability and burning efficiency experiments could be made through various modifications or additions to the COFA and cone setups. Currently, the experiments are conducted under very calm environmental conditions. It has been shown by *in situ* burning field studies, however, that waves and wind can also affect the flammability of crude oil[5,21,36,37]. To simulate such conditions, the COFA could for example be equipped with a wave maker and fans that create a wind over the water surface. Colder climates could be simulated by using a colder cooling medium in the cone setup, similar to Ranellone, *et al*.[20], or by adding ice to water body in the COFA. Finally, the initial thickness of the crude oil slicks can be varied in the experiments, because this is also a parameter known to influence the flammability and burning efficiency of crude oils[5,22].

ACKNOWLEDGMENTS:
The authors would like to thank the Danish Council for Independent research for funding the project (Grant DDF – 1335-00282). COWIfonden funded the construction of the Crude Oil Flammability Apparatus and the gas analyzer, including the duct insert. Maersk Oil and Statoil provided the crude oils that were used for the representative results. None of the sponsors have been involved in the protocol or the results of this paper. The authors would also like to thank Ulises Rojas Alva for assistance with constructing the modified cone sample holder.

DISCLOSURES:
The authors have nothing to disclose.

REFERENCES:
1 Allen, A. A. Contained Controlled Burning of Spilled Oil During the Exxon Valdez Oil Spill. In *Proceedings of the Thirteenth Arctic and Marine Oilspill Program (AMOP) Technical Seminar.* 305-313 (Environment Canada, 1990).
2 Allen, A. A., Jaeger, D., Mabile, N. J. & Costanzo, D. The Use of Controlled Burning During the Gulf of Mexico Deepwater Horizon MC-252 Oil Spill Response. *International Oil Spill Conference Proceedings.* **2011** (1), 1-13, doi:http://dx.doi.org/10.7901/2169-3358-2011-1-194, (2011).
3 AMAP. Assessment 2007: Oil and Gas Activities in the Arctic - Effects and Potential Effects. Vol. 1, 423 (AMAP, Oslo, Norway, 2010).
4 Nuka, Research & Planning Group, LLC. Oil Spill Prevention and Response in the U.S. Arctic Ocean: Unexamined Risks, Unacceptable Consequences. 136 (The PEW Environment

Group, Washington, D.C., 2010).
5 Buist, I. A. *et al.* In Situ Burning in Ice-Affected Waters: State of Knowledge Report. Final Report 7.1.1, 293 (Arctic Response Technology, 2013).
6 EPPR. Guide to Oil Spill Response in Snow and Ice Conditions in the Arctic. 184 (Emergency Prevention Preparedness and Response (EPPR), 2015).
7 Opstad, K. & Guénette, C. Fire on the Sea Surface, Ignitability and Sustainability Under Various Environmental Conditions. *Fire Safety Science.* **6**, 741-752, doi:10.3801/IAFSS.FSS.6-741, (2000).
8 Fritt-Rasmussen, J., Brandvik, P. J., Villumsen, A. & Stenby, E. H. Comparing Ignitability for In Situ Burning of Oil Spills for an Asphaltenic, a Waxy and a Light Crude Oil as a Function of Weathering Conditions Under Arctic Conditions. *Cold Reg. Sci. Technol.* **72**, 1-6, doi:http://dx.doi.org/10.1016/j.coldregions.2011.12.001, (2012).
9 Guénette, C. C. & Thornborough, J. An Assessment Of Two Off-Shore Igniter Concepts. In *Proceedings of the Twentieth Arctic and Marine Oil Spill Program (AMOP) Technical Seminar.* 795-808 (Environment Canada, 1997).
10 Brandvik, P. J., Fritt-Rasmussen, J., Daniloff, R., Leirvik, F. & Resby, J. L. Establishing, testing and verification of a laboratory burning cell to measure ignitability for in situ burning of oil spills. Report No. 20, 26 (SINTEF Materials and Chemistry, Trondheim, 2010).
11 Van Gelderen, L., Malmquist, L. M. V. & Jomaas, G. Vaporization order and burning efficiency of crude oils during in situ burning on water. *Fuel.* **191**, 528-537, doi:http://dx.doi.org/10.1016/j.fuel.2016.11.109, (2017).
12 Farmahini Farahani, H., Shi, X., Simeoni, A. & Rangwala, A. S. A Study on Burning of Crude Oil in Ice Cavities. *Proc. Combust. Inst.* **35** (3), 2699-2706, doi:http://dx.doi.org/10.1016/j.proci.2014.05.074, (2015).
13 Bullock, R. J., Aggarwal, S., Perkins, R. A. & Schnabel, W. Scale-up considerations for surface collecting agent assisted in situ burn crude oil spill response experiments in the Arctic: Laboratory to field-scale investigations. *J. Environ. Manage.* **190**, 266-273, doi:http://dx.doi.org/10.1016/j.jenvman.2016.12.044, (2017).
14 Fingas, M. F. *et al.* The Newfoundland Offshore Burn Experiment - NOBE. In *In Situ Burning Oil Spill Workshop Proceedings.* 63-70 (NIST, 1994).
15 Guénette, C. C. & Wighus, R. In situ Burning of Crude Oil and Emulsions in Broken Ice. In *Proceedings of the Nineteenth Arctic and Marine Oilspill Program (AMOP) Technical Seminar.* 895-906 (Environment Canada, 1996).
16 Potter, S. Tests of Fire-Resistant Booms in Low Concentrations of Drift Ice - Field experiments May 2009. Report No. 27, 17 (SINTEF, Trondheim, 2010).
17 AMAP. Assessment 2007: Oil and Gas Activities in the Arctic - Effects and Potential Effects. Vol. 2, 277 (AMAP, Oslo, Norway, 2010).
18 Buist, I. Window-of-Opportunity for In Situ Burning. *Spill Sci. Technol. Bull.* **8** (4), 341-346, doi:http://dx.doi.org/10.1016/S1353-2561(03)00050-1, (2003).
19 Wu, N., Kolb, G. & Torero, J. L. The Effect of Weathering on the Flammability of a Slick of Crude Oil on a Water Bed. *Combust. Sci. Technol.* **161** (1), 269-308, doi:http://dx.doi.org/10.1080/00102200008935820, (2000).
20 Ranellone, R. T., Tukaew, P., Shi, X. & Rangwala, A. S. Ignitability of crude oil and its oil-in-water products at arctic temperature. *Mar. Pollut. Bull.* **115** (1), 261-265,

doi:http://dx.doi.org/10.1016/j.marpolbul.2016.12.021, (2017).

21 Bech, C. M., Sveum, P. & Buist, I. A. The Effect of Wind, Ice and Waves on the In situ Burning of Emulsions and Aged Oils. In *Proceedings of the Sixteenth Arctic and Marine Oilspill Program (AMOP) Technical Seminar.* 735-748 (Environment Canada, 1993).

22 Van Gelderen, L. *et al.* Importance of the Slick Thickness for Effective In situ Burning of Crude Oil. *Fire Saf. J.* **78**, 1-9, doi:http://dx.doi.org/10.1016/j.firesaf.2015.07.005, (2015).

23 ISO 17554:2014(E) Reaction to fire tests – Mass loss measurement. 28 (International Organization for Standardization, Geneva, 2014).

24 ISO/TR 9705-2:2001(E) Reaction-to-fire tests – Full-scale room tests for surface products – Part 2: Technical background and guidance. 39 (International Organization for Standardization, Geneva, 2001).

25 Stiver, W. & Mackay, D. Evaporation rate of spills of hydrocarbons and petroleum mixtures. *Environ. Sci. Technol.* **18** (11), 834-840, doi:http://dx.doi.org/10.1021/es00129a006, (1984).

26 Buist, I., Potter, S., Zabilansky, L., Guarino, A. & Mullin, J. in *Oil Spill Response: A Global Perspective,* (eds W. F. Davidson, K. Lee, & A. Cogswell) 41-62 (Springer Netherlands, 2008).

27 Daling, P. S., Moldestad, M. Ø., Johansen, Ø., Lewis, A. & Rødal, J. Norwegian Testing of Emulsion Properties at Sea—The Importance of Oil Type and Release Conditions. *Spill Sci. Technol. Bull.* **8** (2), 123-136, doi:http://dx.doi.org/10.1016/S1353-2561(03)00016-1, (2003).

28 Arai, M., Saito, K. & Altenkirch, R. A. A Study of Boilover in Liquid Pool Fires Supported on Water Part I: Effects of a Water Sublayer on Pool Fires. *Combust. Sci. Technol.* **71** (1-3), 25-40, doi:http://dx.doi.org/10.1080/00102209008951622, (1990).

29 Garo, J. P., Vantelon, J. P. & Fernandez-Pello, A. C. Boilover Burning of Oil Spilled on Water. *Symp. (Int.) Combust.* **25** (1), 1481-1488, doi:http://dx.doi.org/10.1016/S0082-0784(06)80792-7, (1994).

30 Evans, D. D., Mulholland, G. W., Gross, H., Baum, H. & Saito, K. Burning, smoke production, and smoke dispersion from oil spill combustion. In *Proceedings of the Eleventh Arctic and Marine Oilspill Program (AMOP) Technical Seminar.* 41-87 (Environment Canada, 1988).

31 Guénette, C. C., Sveum, P., Buist, I., Aunaas, T. & Godal, L. In situ burning of water-in-oil emulsions. 139 (Marine Spill Response Corporation, Washington D.C., 1994).

32 Van Gelderen, L., Rojas Alva, U., Mindykowski, P. & Jomaas, G. Thermal Properties and Burning Efficiencies of Crude Oils and Refined Fuel Oil. *International Oil Spill Conference Proceedings.* **2017** (1), 985-1005, doi:10.7901/2169-3358-2017.1.985, (2017).

33 Quintiere, J. G. in *Fundamentals of Fire Phenomena,* Ch. 7, 159-190 (John Wiley & Sons, Ltd, 2006).

34 Janssens, M. L. Measuring rate of heat release by oxygen consumption. *Fire Technol.* **27** (3), 234-249, doi:http://dx.doi.org/10.1007/bf01038449, (1991).

35 Brandvik, P. J. & Faksness, L.-G. Weathering processes in Arctic oil spills: Meso-scale experiments with different ice conditions. *Cold Reg. Sci. Technol.* **55** (1), 160-166, doi:http://dx.doi.org/10.1016/j.coldregions.2008.06.006, (2009).

36 Wighus, R. & Guènette, C. Fire on the sea surface - Experiments hazard assessment 1995. Report No. NBL A07129, 40 (SINTEF, Trondheim, 2007).

37 Guénette, C. C., Sveum, P., Bech, C. M. & Buist, I. A. Studies of In Situ Burning of Emulsions in Norway. *International Oil Spill Conference Proceedings.* **1995** (1), 115-122, doi:http://dx.doi.org/10.7901/2169-3358-1995-1-115, (1995).

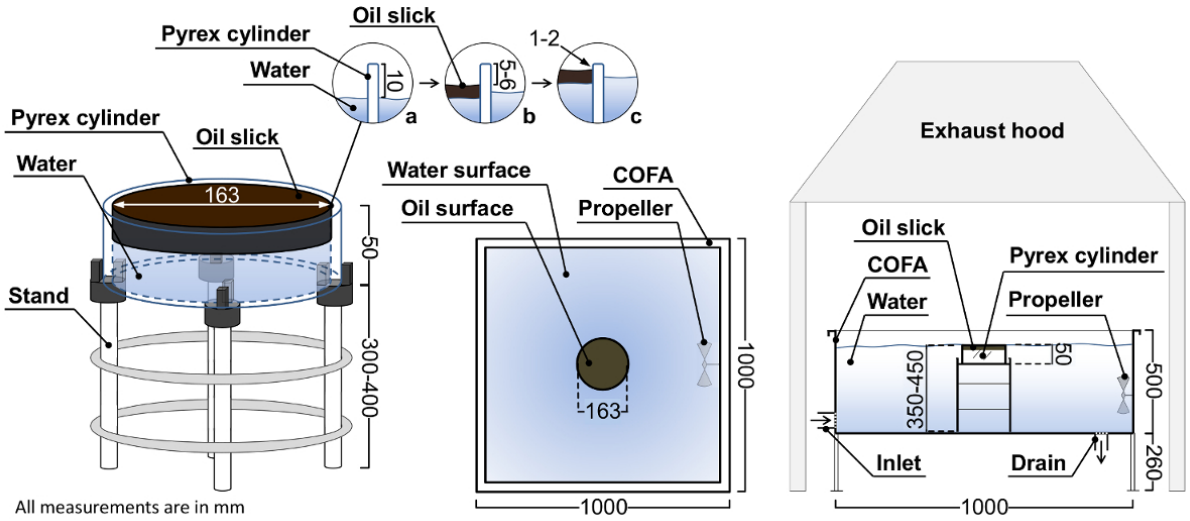

Figure 1

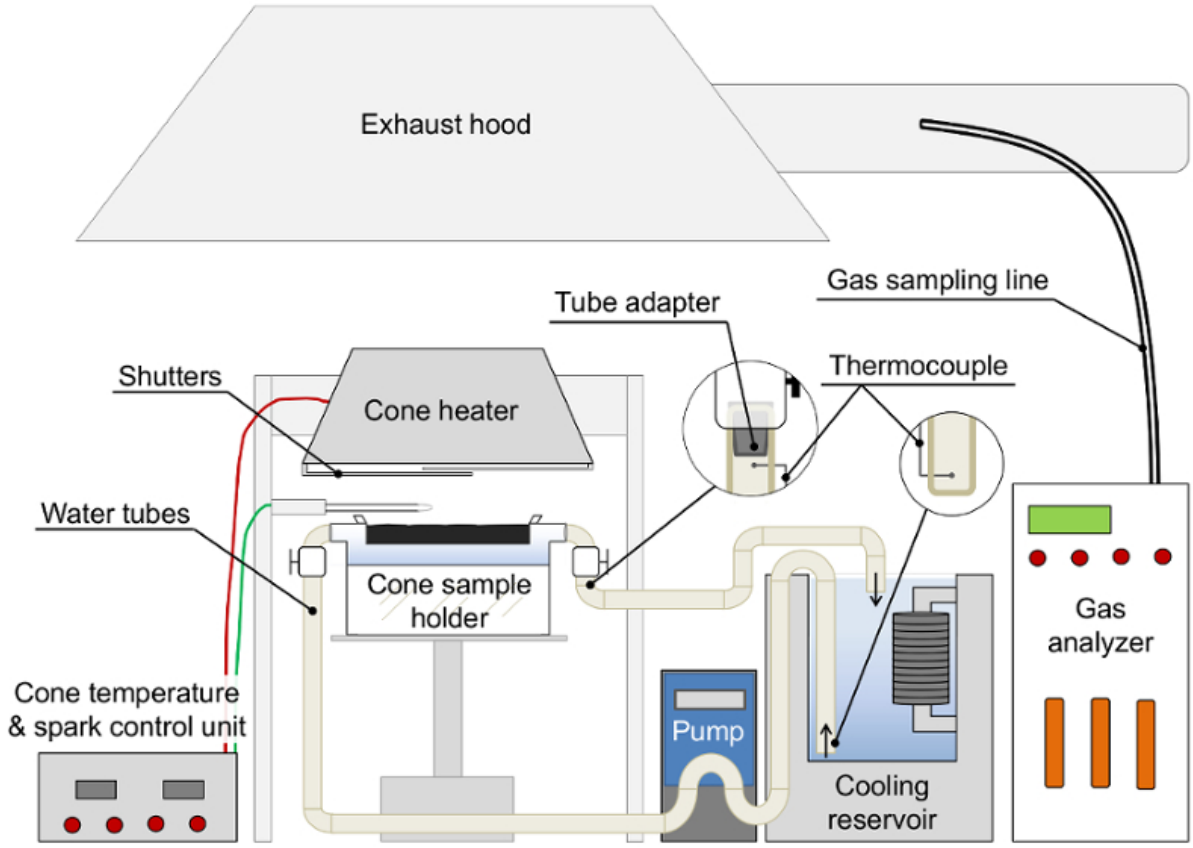
Exhaust hood
Gas sampling line
Tube adapter
Thermocouple
Shutters
Cone heater
Water tubes
Cone sample holder
Gas analyzer
Cone temperature & spark control unit
Pump
Cooling reservoir

Figure 2

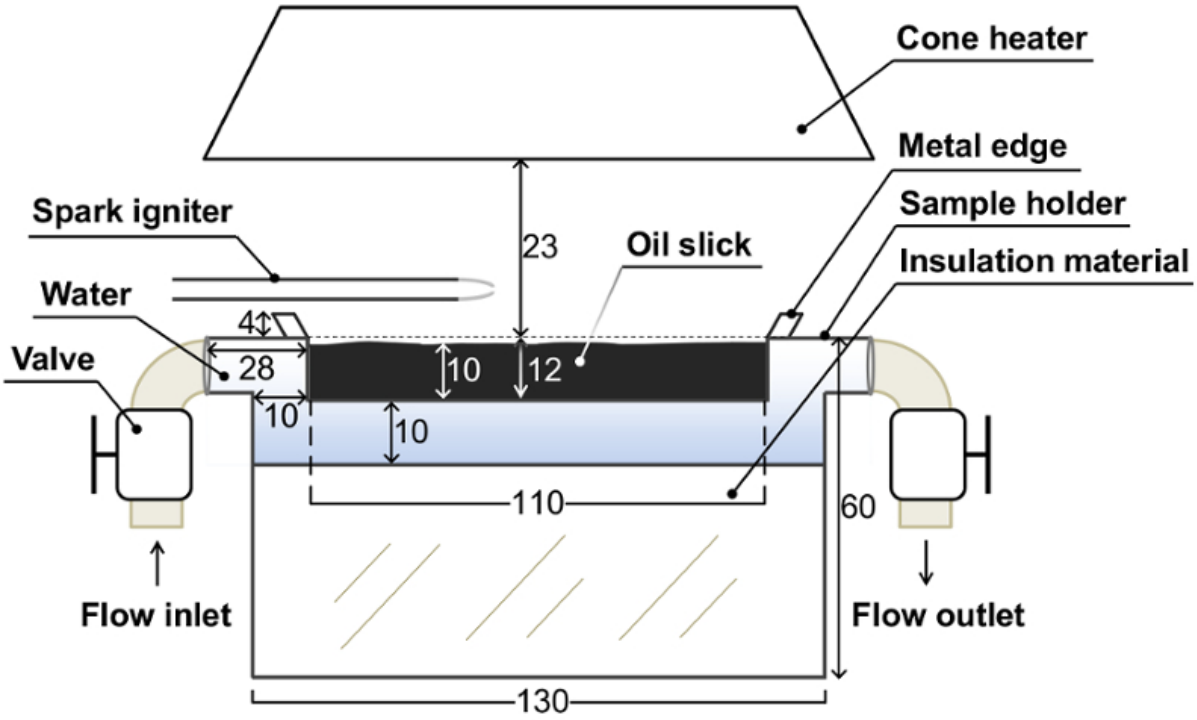

All measurements are in mm

Figure 3

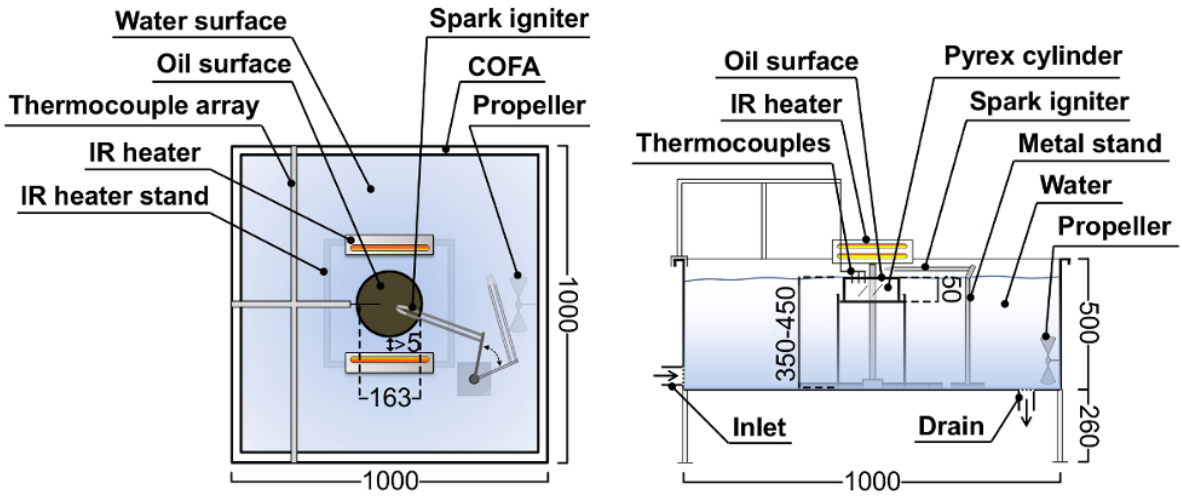

All measurements are in mm

Figure 4

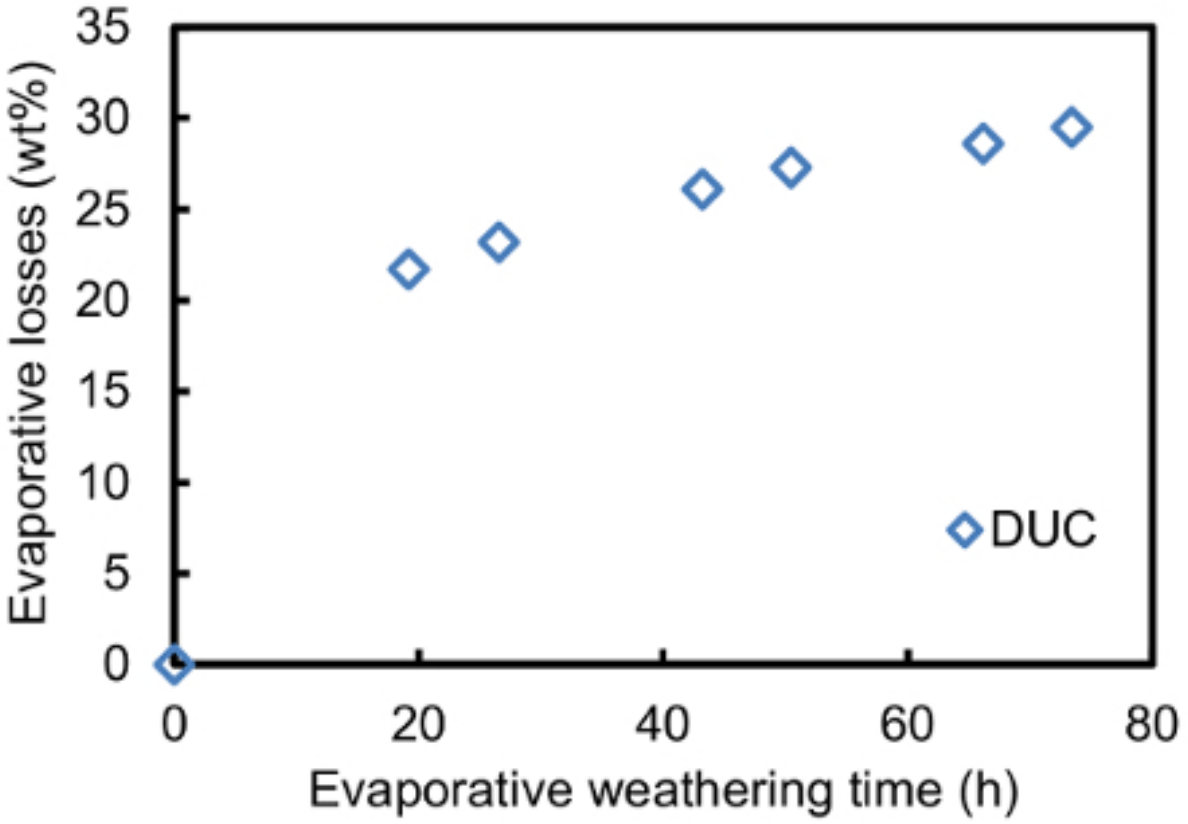

Figure 5

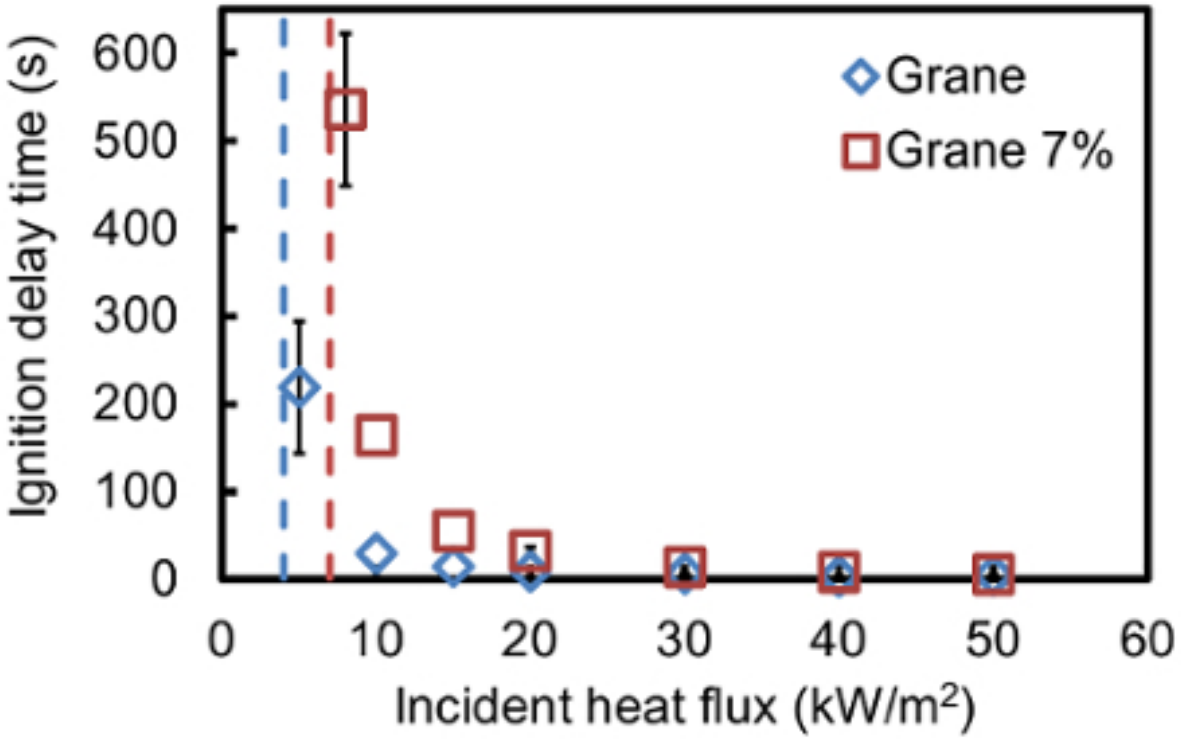

Figure 6

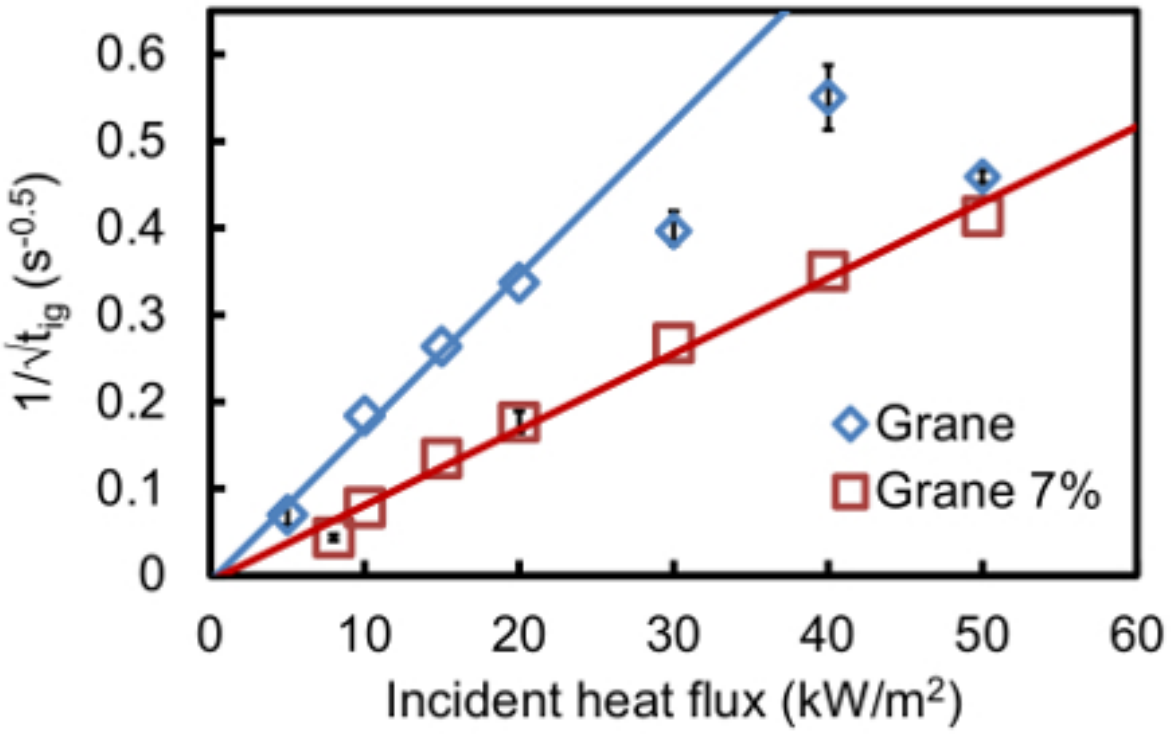

Figure 7

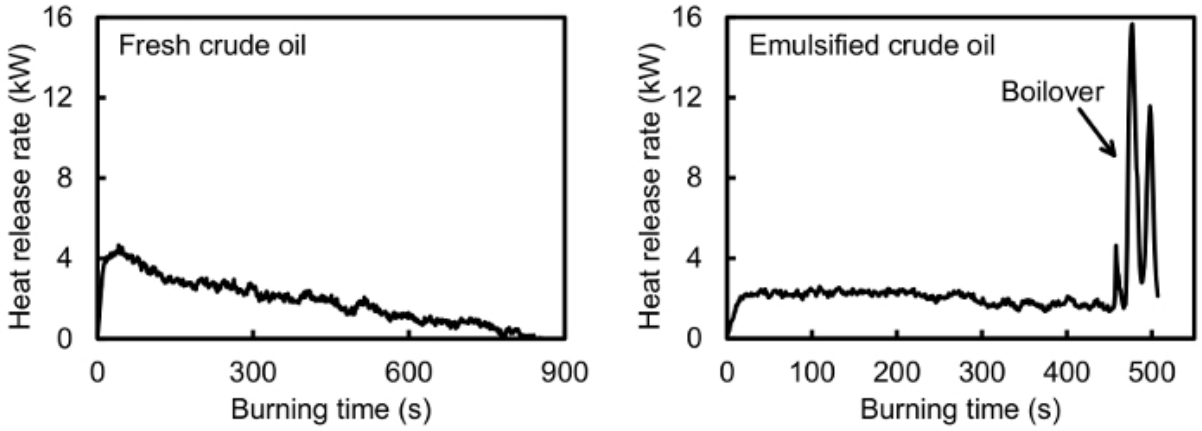

Figure 8

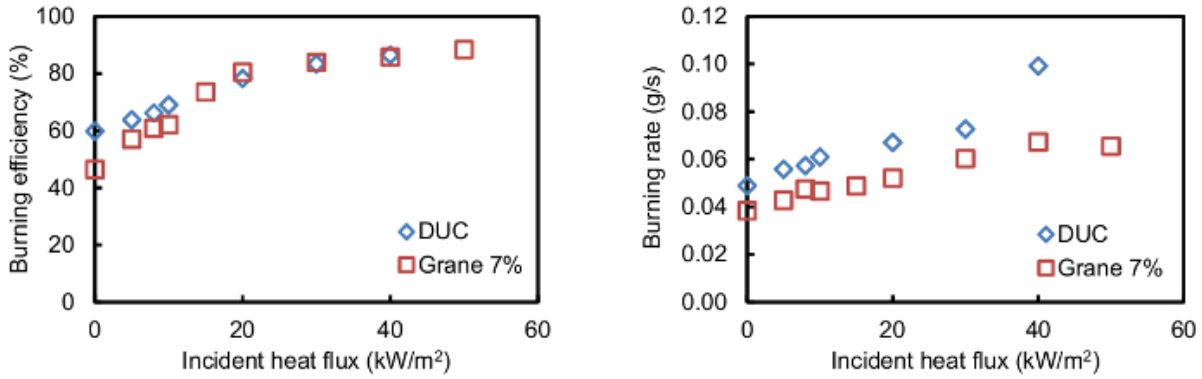

Figure 9

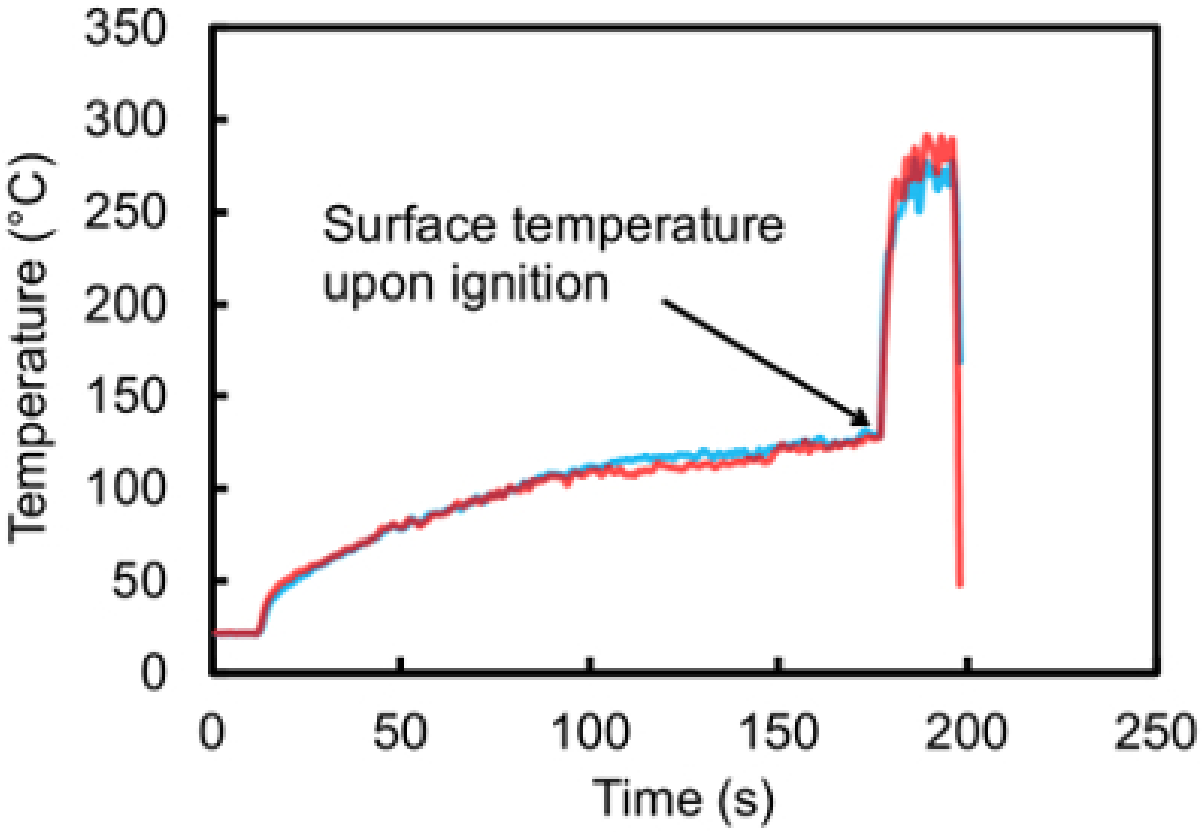

Figure 10

SUPPLEMENTARY DOCUMENT

Title: Experimental procedure for laboratory studies of *in-situ* burning – flammability and burning efficiency of crude oil

AUTHORS & AFFILIATIONS:
Laurens van Gelderen[1] and Grunde Jomaas[1,2]
[1] *Department of Civil Engineering, Technical University of Denmark, Kgs. Lyngby, Denmark*
[2] *School of Engineering, BRE Centre for Fire Safety Engineering, University of Edinburgh, Edinburgh, United Kingdom*

Corresponding Author:
Laurens van Gelderen
Email Address: lauge@byg.dtu.dk
Tel: (0045) – 4525 1808

Email Addresses of Co-authors**:**
Grunde Jomaas (Grunde.Jomaas@ed.ac.uk)

S.1. Crude Oil Flammability Apparatus (COFA) (Figs. 1, 4 and S1)
The COFA is a stainless steel water basin of 1.0 x 1.0 x 0.50 m^3 featuring two opposite walls with glass windows of 0.86 x 0.37 m^2 for additional observation capabilities of the oil-water interface. It stands on four stainless steel feet with a height of 0.26 m. The top edges of the COFA are extended to a width of 5 cm, so that extensions can be placed on the COFA such as the holder for the surface temperature thermocouples (Fig. 4). An inlet connection for water is attached to one of the metal side walls near the bottom plate and a drain is attached to the bottom plate.

The exhaust hood directly above the COFA has an intake area of 1.5 x 1.5 m^2 and is placed on four legs of 0.07 x 0.07 x 2.05 m^3. The exhaust area is located 2.3 m above the bottom of the COFA and has an area of 0.50 x 0.16 m^2. Air is extracted with a velocity of 6.8-8.4 m/s or 8.4-10.4 m/s (higher velocities are used for more sooty fires) and the combustion gases are discharged through a connected exhaust duct with a diameter of 0.21 m.

The infrared (IR) heaters that are used in the COFA for the surface temperature upon ignition are modified versions of the standard M110 modules provided by their manufacturer (see the Materials/Equipment table). These heaters consist of two short wave twin tube emitters (heating elements) with a total radiative power of 1.9 kW and a heated length of 0.20 m. The backside of these heating elements is coated with a thin gold layer to redirect radiation towards the front of the heater and as such amplify the effective output of the heaters. The temperature of this part of the heating element should not exceed 500 °C in order to preserve its gold layer. In the original design, the casing and heating elements are cooled by a fan that sucks in cold air from the back of the heater and blows it through the heater in the same direction as the heating direction. In order to avoid the air flow from the cooling fan from

reaching the oil surface, a custom-made water-cooled holder was designed for the two heating elements. This water-cooled holder functions as an alternative cooling method for the heating elements while blocking the air flow from the fan. A schematic overview of the modified heaters is shown in Fig. 1S.

Water is pumped through the IR heaters using an aquarium pump (with an adjustable flow) in a basin with at least 20 L of water. The pump and IR heaters are connected with plastic tubes with an internal diameter of 4-10 mm. At maximum power, the gold-coated backside of the heating elements should stabilize at a maximum temperature of about 450 °C and the water flow should be calibrated accordingly. To calibrate the cooling of the IR heaters, place the heaters in an initial position in the COFA (*i.e.* opposite of each other and approximately 5 cm from the Pyrex glass cylinder as in Step 8.1). Place a 1 mm thick K-Type thermocouple between the backside of each heating element and the water-cooled holder and connect the thermocouples to a data logger. Start the data logger, turn on the pump and turn on the IR heaters. Carefully increase the power output percentage while monitoring the temperature of the heating elements. If the measured temperatures reach above 450 °C, turn down the power output of the IR heaters, increase the water flow and start increasing the power output of the IR heaters again. Once the backsides of the heating elements reach a stable temperature of 450 °C for at least 15 minutes at maximum power, the corresponding water flow is the calibrated flow that should be used during all experiments. It should be noted that the front of the heating elements may be much hotter than its backside (> 600 °C). Ensure therefore that the glass type of the heating elements is resistant to high temperature gradients.

In the COFA setup, each IR heaters is, through its custom-made housing, attached to a stainless steel tube of 0.03 x 0.03 x 0.40 m^3. The angle between the IR heater clamp and its connected tube is fully adjustable so that the IR heater can be placed to face the Pyrex glass cylinder from any angle between 0-90 °. Each stainless steel tubes slides into another stainless steel tube of 0.04 x 0.04 x 0.20 m^3 that is attached to a metal foot, which is placed freely in the COFA. The height of the tube attached to the heater clamp inside the other tube is freely adjustable, so that the distance between the metal foot and IR heater can be varied between 0.40-0.60 m. This highly flexible setup for the IR heaters relative to the Pyrex glass cylinder is an important feature of the COFA because it is used to ensure an incident heat flux to the oil surface that will result in ignition.

S.2. Cone heater with gas analyzer (Figs. 2, 3 and S2).

The cone heater that is used in Steps 5-7 is a standard mass loss calorimeter, as described in ISO 17554[1], apart from the custom-made circular sample holder (Fig. 3). The full cone setup (Fig. 2) is placed on a 0.90 m high table under the exhaust hood. The exhaust hood used in connection with the cone setup has an intake area of 2.6 x 2.6 m^2 and is placed on four legs of 0.10 x 0.10 x 2.0 m^3. The exhaust area is located at a height of 3.4 m from the floor in the center of the hood and is connected to an exhaust duct with a diameter of 0.315 m. Air is extracted with a velocity of approximately 6 m/s. The exhaust duct is equipped with a duct insert that includes the sampling probes, pressure transducer, thermocouples and a laser (which are part of the gas analyzer) at a distance of 3.26 m from the duct inlet. In addition to measuring the O_2, CO_2 and

CO concentrations in the exhaust gases, the duct insert is used to measure the temperature of the exhaust gases and the pressure difference created by the suction of the hood. An additional, separate thermocouple was suspended in the air in the laboratory to measure the ambient temperature. These six measurements are used to calculate the heat release rate as described below. More details on the gas analyzer can be found in ISO/TR 9705-2[2].

S.3. Calculation method for the heat release rate based on O_2, CO_2 and O_2 concentrations.

The calculation method for the heat release rate as described by Janssens [3] was used to obtain the shown heat release rate results in Fig. 8. This method has also been included in ISO/TR 9705-2[2]. Here, a concise overview of the assumptions and equations from Janssens [3] is given that can be used to calculate the heat release rate based on the acquired data from the gas analyzer. For a more detailed discussion of this method, see Janssens [3].

The following equations are used, in order, to calculate the heat release rate. A description of all the terms and symbols in these equations, including relevant assumptions and the acquisition methods, is provided below.

$$\dot{m}_e = \frac{A \cdot k_c}{f(RE)} \sqrt{\frac{\Delta p}{T_e}} \tag{S1}$$

$$\ln(p_s) = 23.2 - 3816/(-46 + T_a) \tag{S2}$$

$$X^{\circ}_{H_2O} = \frac{RH}{100} \frac{p_s}{p_a} \tag{S3}$$

$$M_a = M_{dry}\left(1 - X^{\circ}_{H_2O}\right) + M_{H_2O} \cdot X^{\circ}_{H_2O} \tag{S4}$$

$$\phi = \frac{X^{A^{\circ}}_{O_2}\left(1 - X^{A}_{CO_2} - X^{A}_{CO}\right) - X^{A}_{O_2}\left(1 - X^{A^{\circ}}_{CO_2}\right)}{\left(1 - X^{A}_{O_2} - X^{A}_{CO_2} - X^{A}_{CO}\right) X^{A^{\circ}}_{O_2}} \tag{S5}$$

$$\dot{q} = \left[E\phi - (E_{CO} - E)\frac{1 - \phi}{2}\frac{X^{A}_{CO}}{X^{A}_{O_2}}\right] \frac{\dot{m}_e}{1 + \phi(\alpha - 1)} \frac{M_{O_2}}{M_a} \left(1 - X^{\circ}_{H_2O}\right) X^{A^{\circ}}_{O_2} \tag{S6}$$

In Eq. (S1), the area of the duct (A) in is 0.078 m^2, the velocity profile shape factor (k_c) was assumed to be 0.9 (*i.e.* close to unity) and the Reynolds number correction ($f(RE)$) is taken as 1.08. The pressure difference (Δp) is measured in volt by the pressure transducer in the duct insert and converted to pascal by using the calibration points that are provided by the manufacturer. Finally, the temperature of the exhaust gases (T_e) is directly measured by a thermocouple in the duct insert.

The saturation pressure (p_s) in Eq. (S2) is calculated based on a set of constants and the measured ambient temperature (T_a). This number is then used in Eq. (S3) to calculate the mole fraction of water in the ambient air ($X^{\circ}_{H_2O}$), in combination with the relative humidity (RH) and

the ambient pressure (p_a), which is taken as 101,325 Pa (1 atm). The relative humidity (in %) is typically obtained through a weather forecast and was taken as 60% for the data shown in Fig. 8. It should be noted that the Eq. (S6) is very insensitive towards the relative humidity and that the accuracy of the weather forecast is thus insignificant with respect to the final calculated heat release rate. The molar mass of the ambient air (M_a) in Eq. (S4) can then be calculated by taking the molar masses for dry air (M_{dry}) and water (M_{H_2O}) as 29 and 18 kg/kmol, respectively.

The calculation method for the oxygen depletion factor (ϕ) depends on which gas concentrations in the exhaust gases are measured by the gas analyzer. For gas analyzers that measure O_2, CO_2 and CO, the oxygen depletion factor is calculated with Eq. (S5). In this equation, $X_{O_2}^{A^\circ}$ and $X_{CO_2}^{A^\circ}$ are the measured molar fraction of oxygen and carbon dioxide, respectively, in the ambient air. This measurement is typically obtained at the start of an experiment between the period that the data logger is started and the crude oil sample is actually subjected to incident heat flux from the cone heater. The remaining terms in this equation consist of the measured concentrations of O_2, CO_2 and CO in the exhaust gases during the experiment ($X_{O_2}^{A}$, $X_{CO_2}^{A}$ and X_{CO}^{A}, respectively).

The heat release rate ($\dot{q}$) can then be calculated with Eq. (S6), based on the calculated terms in the previous equations and a set of constants. The used calculation method assumes a constant value for the net heat release rate per unit mass of oxygen consumed (E) and for the net heat release rate per unit mass of oxygen consumed for the combustion of CO to CO_2 (E_{CO}). These values are taken as 13,100 and 17,600 kJ/kg of O_2, respectively. The combustion expansion factor (α) is taken as 1.105. By calculating the heat release rate for all measurements taken during the experiment, the heat release rate is as such calculated as a function of time, as shown in Fig. 8.

FIGURE AND TABLE LEGENDS:

Figure S1. Photos of the COFA setup (top left), a close-up view of the Pyrex glass cylinder with the water surface approximately 1 cm below the cylinder edge (top right), the COFA setup including two unmodified IR heaters, the spark igniter and the thermocouples to measure the surface temperature of the oil (bottom left) and a close-up of the spark igniter and thermocouples above the Pyrex glass cylinder (bottom right). These photos are intended to give a visual impression of the experimental setups and cannot be used as a replacement of the setup schematics (Figs. 1 and 4)

Figure S2. Photos of the plastic container including the O-ring for the evaporative weathering of crude oil (top left, Step 2), an overview of the cone setup featuring the control unit, cone heater, sample holder, water cooling reservoir and peristaltic pump (top right), close-up of the cone heater with the sample holder (bottom left) and a close-up of the sample holder (bottom right). These photos are intended to give a visual impression of the experimental setups and cannot be used as a replacement of the setup schematics (Figs. 2 and 3).

Figure S3. Schematics of the modified IR heater showing a top view (top left), front view (bottom left) and the respective cross-section side views (right).

REFERENCES

1 ISO 17554:2014(E) Reaction to fire tests – Mass loss measurement. 28 (International Organization for Standardization, Geneva, 2014).

2 ISO/TR 9705-2:2001(E) Reaction-to-fire tests – Full-scale room tests for surface products – Part 2: Technical background and guidance. 39 (International Organization for Standardization, Geneva, 2001).

3 Janssens, M. L. Measuring Rate of Heat Release by Oxygen Consumption. *Fire Technol.* **27** (3), 234-249, doi:http://dx.doi.org/10.1007/bf01038449, (1991).

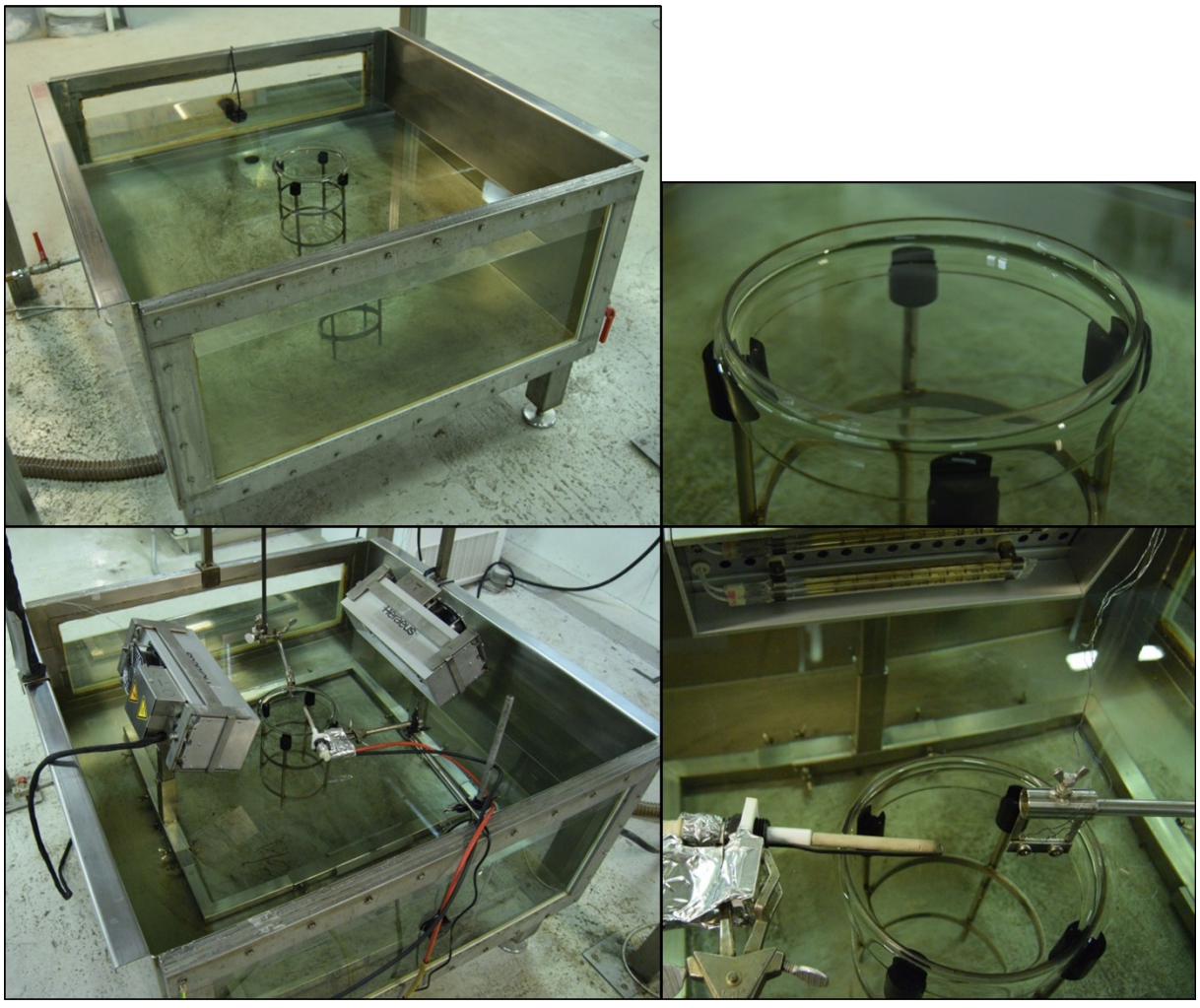

Figure S1

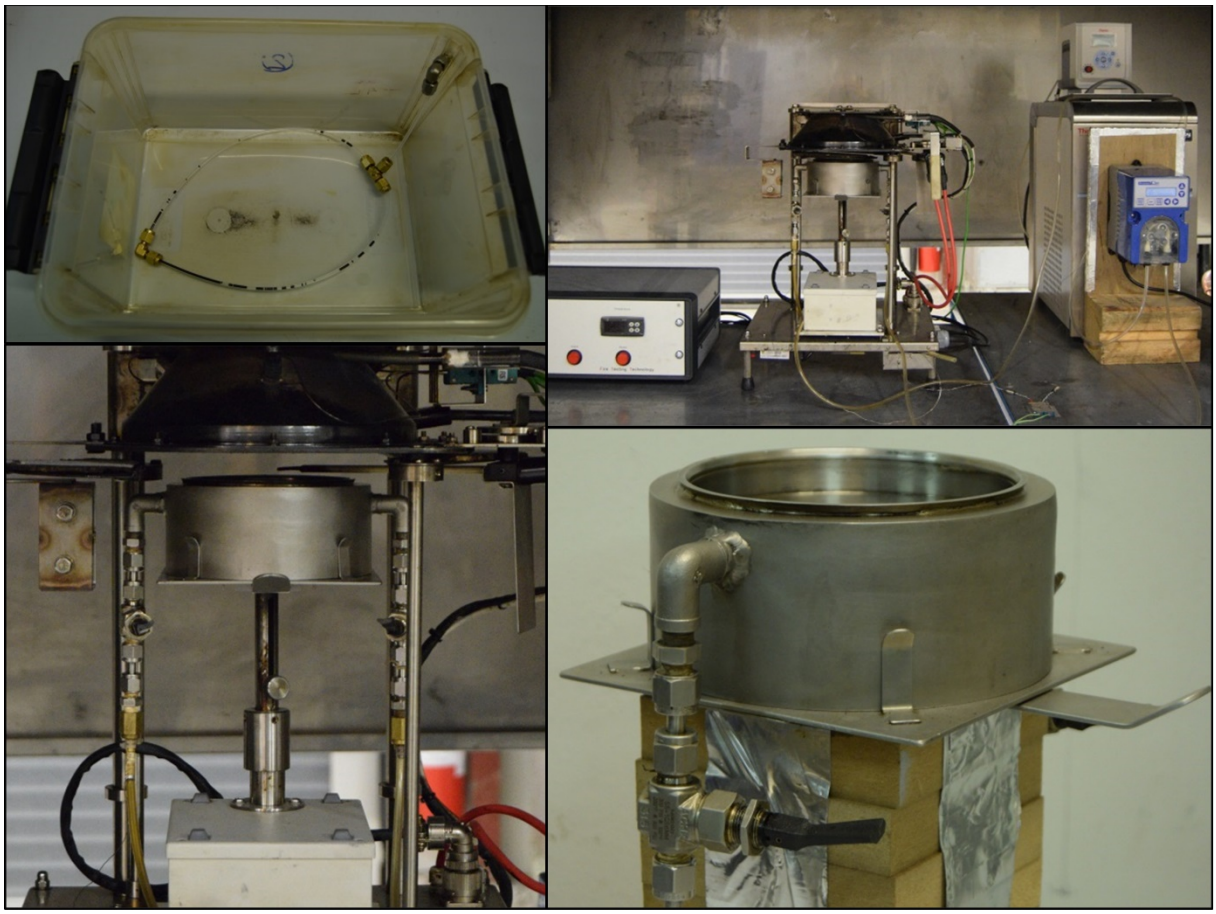

Figure S2

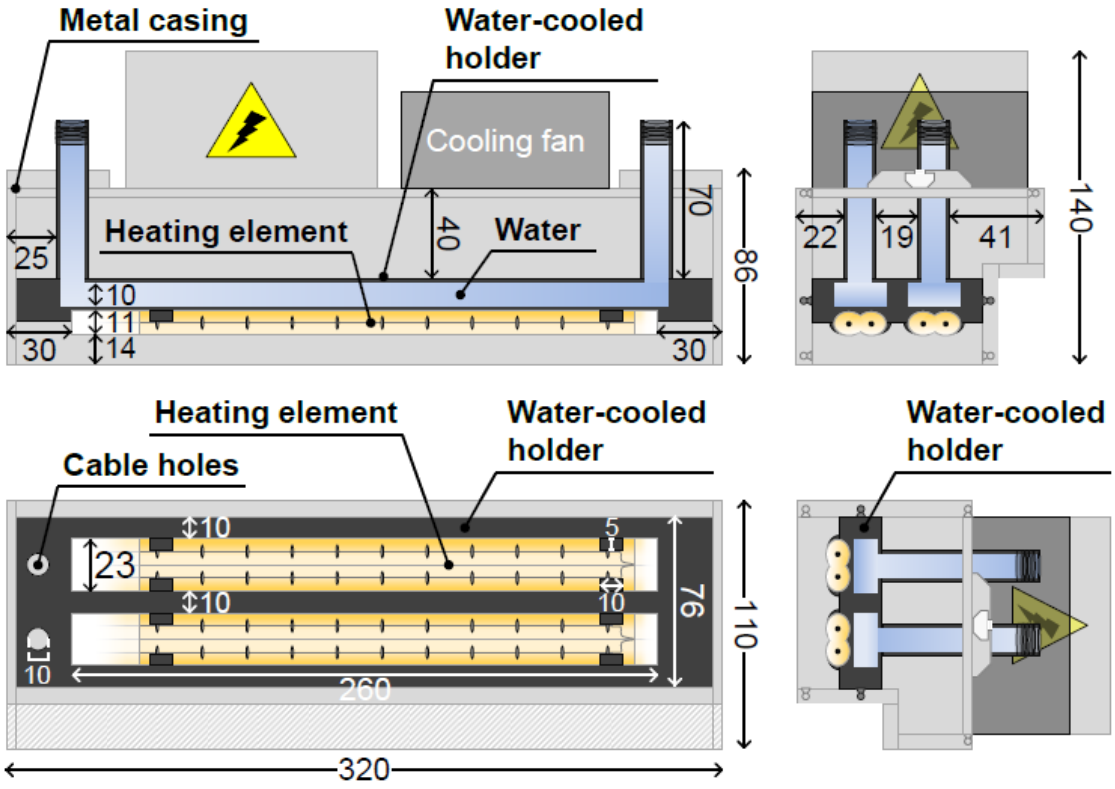
Metal casing
Water-cooled holder
Cooling fan
Heating element
Water
25
40
70
86
10
11
14
30
30
22
19
41
140
Heating element
Water-cooled holder
Water-cooled holder
Cable holes
23
10
10
10
5
10
76
110
260
320

Figure S3